Journal of Hazardous Materials 196 (2011) 380–385

Contents lists available at SciVerse ScienceDirect

Journal of Hazardous Materials

journal homepage: www.elsevier.com/locate/jhazmat

The roles of various plasma species in the plasma and plasma-catalytic removal of low-concentration formaldehyde in air

Xing Fan, Tianle Zhu*, Yifei Sun, Xiao Yan

School of Chemistry and Environment, Beihang University, No. 37 Xueyuan Road, Haidian District, Beijing 100191, China

ARTICLE INFO

Article history:
Received 5 May 2011
Received in revised form 9 September 2011
Accepted 10 September 2011
Available online 16 September 2011

Keywords:
Formaldehyde
Discharge plasma
MnO_x/Al_2O_3 catalyst
Plasma-catalysis
Ozone

ABSTRACT

The contributions of various plasma species to the removal of low-concentration formaldehyde (HCHO) in air by DC corona discharge plasma in the presence and absence of downstream MnO_x/Al_2O_3 catalyst were systematically investigated in this study. Experimental results show that HCHO can be removed not only by short-living active species in the discharge zone, but also by long-living species except O_3 downstream the plasma reactor. O_3 on its own is incapable of removing HCHO in the gas phase but when combined with the MnO_x/Al_2O_3 catalyst, considerable HCHO conversion is seen, well explaining the greatly enhanced HCHO removal by combining plasma with catalysis. The plasma-catalysis hybrid process where HCHO is introduced through the discharge zone and then the catalyst bed exhibits the highest energy efficiency concerning HCHO conversion, due to the best use of plasma-generated active species in a two-stage HCHO destruction process. Moreover, the presence of downstream MnO_x/Al_2O_3 catalyst significantly reduced the emission of discharge byproducts (O_3) and organic intermediates (HCOOH).

1. Introduction

Low-concentration formaldehyde (HCHO), mainly originating from furnishing and building materials, widely exists in indoor environments, and has been correlated to adverse health effects such as eye, nose and throat irritation, allergic asthma, pulmonary function damage and even cancer [1–3]. Conventional technologies, such as adsorption, catalytic and photo-catalytic oxidation, have been widely investigated for the removal of HCHO [4–9]. Complete oxidation of 100-ppm HCHO was achieved over a Pt/TiO_2 catalyst even at room temperature [6]. However, the limited removal capacities of adsorbent materials and the expensive cost of noble metals still limit their widespread applications.

As an alternative approach, non-thermal plasma (NTP) technology is likely to be more appropriate for indoor air purification because it is capable of removing various indoor pollutants such as particulate matters, bacteria and volatile organic compounds (VOCs) simultaneously under ambient conditions. Atmospheric plasma discharges generate high-energy electrons, while the background gas remains close to room temperature. The energetic electrons excite, dissociate and ionize gas molecules, producing chemically active species for removal of VOCs [10].

NTP process alone, however, has disadvantages such as high energy consumption, poor selectivity towards total oxidation and undesired byproduct formation [11–13]. An attempt to overcome these disadvantages is to combine plasma technology with heterogeneous catalysis [10,14–18]. Fan et al. [17] reported that the BTX (mixture of benzene, toluene and *p*-xylene) conversion can be greatly enhanced by introducing MnO_x/Al_2O_3 catalyst after the discharge zone, at the same time harmful O_3 can be removed from the exit gas stream.

On the other hand, despite the excellent performance of the plasma-catalysis hybrid process [19], the underlying mechanisms involved in the plasma-catalytic destruction of VOCs are not well understood yet. Since various active species, such as energetic electrons, radicals, ions, stable and metastable molecules/atoms, coexist in the discharge plasma, the study of the contributions of these species to the removal of VOCs can bring valuable information about the destruction processes. Harling et al. [20] investigated the role of O_3 in the destruction of toluene and cyclohexane using the combination of NTP with either MnO_2 or MnO_2–CuO catalyst. It was deduced that the decomposition of O_3 to active oxygen species over the catalyst surface initiated heterogeneous destruction reactions, leading to complete removal of toluene and cyclohexane.

In the present study, different plasma and plasma–catalyst hybrid systems were designed for the removal of low-concentration HCHO in air. A link tooth wheel-cylinder energized by positive DC high voltage was used as the plasma reactor while MnO_x/Al_2O_3 was selected as the post-plasma catalyst. The main objective of this work is to investigate the roles of different plasma species in the conversion of HCHO, both in the gas phase and over the catalyst surface. Besides, the energy efficiency concerning

* Corresponding author. Tel.: +86 10 82314215; fax: +86 10 82314215.
E-mail address: zhutl@buaa.edu.cn (T. Zhu).

0304-3894/$ – see front matter © 2011 Elsevier B.V. All rights reserved.
doi:10.1016/j.jhazmat.2011.09.044

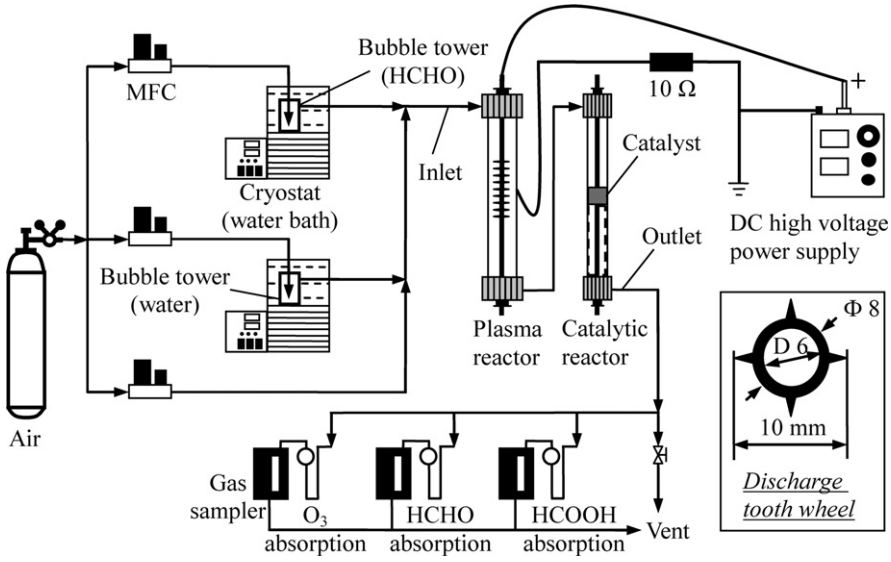

Fig. 1. Schematic diagram of the experimental set-up.

HCHO conversion, and the behavior of byproduct formation, including O_3 and organic byproducts, were also investigated for the plasma and plasma-catalysis hybrid processes.

2. Experimental

2.1. Experimental set-up

A schematic diagram of the experimental system is shown in Fig. 1. It consists of a tandem plasma–catalyst reactor system, a 25 kV/5 mA positive DC high voltage power supply, reaction gas supply and analytical instrumentation. A stainless steel cylinder with an inner diameter of 42 mm was used as the ground electrode of the plasma reactor, while a stainless steel rod (o.d. 6 mm) through which 9 discharge teeth wheels were linked with a space interval of 10 mm was used as the high voltage electrode. The effective discharge length and discharge gap were 89 and 16 mm, respectively. A stainless steel cylinder with an inner diameter of 27 mm was connected to the link tooth wheel-cylinder plasma reactor in series, in order to construct a plasma–catalyst hybrid system or a plasma alone system by introducing the MnO_x/Al_2O_3 catalyst or not.

In order to investigate the roles of different plasma species in the conversion of HCHO, six treatment systems with different gas-feeding methods or configurations were designed, as shown in Fig. 2. Treatment systems A–C were constructed for homogeneous reaction of HCHO while systems D–F also included heterogeneous reactions over the MnO_x/Al_2O_3 catalyst. HCHO was introduced before the plasma in systems A and D, while in other systems HCHO was directly introduced into the post-plasma cylinder. In systems C and F, a buffer flask with capacity of 7 L (gas residence time of 70 s) was inserted between the two cylinders in order to extinguish active species from the plasma except O_3 (O_3 has a lifetime of several days at room temperature).

2.2. Experimental methods

Gaseous HCHO and water vapor were introduced by passing dry air through two temperature-controlled bubble towers, containing 36 wt.% HCHO solution and deionized water, respectively. The water vapor was first mixed with the dilution air and then with the gaseous HCHO before or after the plasma reactor (Fig. 2). The flow rates of air were controlled by a set of mass flow controllers and the total flow rate of the reaction gas was controlled at 6.0 L/min. The initial HCHO concentration and relative humidity (RH) of the reaction gas were 2.2 ± 0.1 ppm and $30 \pm 3\%$, respectively. All the tests were carried out at room temperature and atmospheric pressure.

MnO_x/Al_2O_3 (5 wt.% Mn) prepared by the impregnation method, with manganese acetate as the precursor and γ-Al_2O_3 of 2.5–3.5 mm in diameter as the support, was used as the catalyst in this study [17]. Loading amount of the catalyst was 15.0 g, with the residence time in the catalyst bed being around 0.21 s. When the catalyst was introduced, the reaction was started by energizing the plasma reactor with DC only when the HCHO concentration at the exit of the catalytic reactor reached a steady state, meaning that initial adsorption–desorption equilibrium of HCHO over the catalyst surface was achieved.

HCHO, HCOOH and O_3 were sampled at the exit of the catalytic reactor and then analyzed by acetylacetone spectrophotometric method [21], ion chromatography (ICS200; Dionex Corporation, USA), and indigo disulphonate spectrophotometric method [17], respectively. HCHO and HCOOH were absorbed by distilled water while O_3 by the solution of indigo disulphonate. The conversion of HCHO and the yield of HCOOH are defined as follows.

$$\eta_{HCHO}\ (\%) = \frac{[HCHO]_{off} - [HCHO]_{on}}{[HCHO]_{off}} \times 100 \quad (1)$$

$$Y_{HCOOH}\ (\%) = \frac{[HCOOH]}{[HCHO]_{off} - [HCHO]_{on}} \times 100 \quad (2)$$

where $[HCHO]_{on}$ and $[HCHO]_{off}$ denote the concentrations of HCHO (ppm) at the exit of the catalytic reactor with the power supply for the plasma reactor being on and off; and [HCOOH] is the concentration of HCOOH (ppm) measured at the exit of the catalytic reactor.

The energy efficiency concerning HCHO conversion (η_E, the removed amount of HCHO per kWh of energy consumption, g/kWh) was also evaluated in this study to determine the capability of the treatment processes for practical applications. Since the specific input energy (SIE, the discharge energy deposited into 1 L of reaction gas, J/L) directly reflects the energy consumption of the plasma discharge, all the experimental results were compared on the basis of SIE in this investigation. SIE and η_E are calculated as follows.

$$SIE = \frac{UI}{Q} \times 60 \quad (3)$$

$$\eta_E = \frac{[HCHO]_{off} - [HCHO]_{on}}{SIE} \times \frac{30 \times 3.6}{24.4} \quad (4)$$

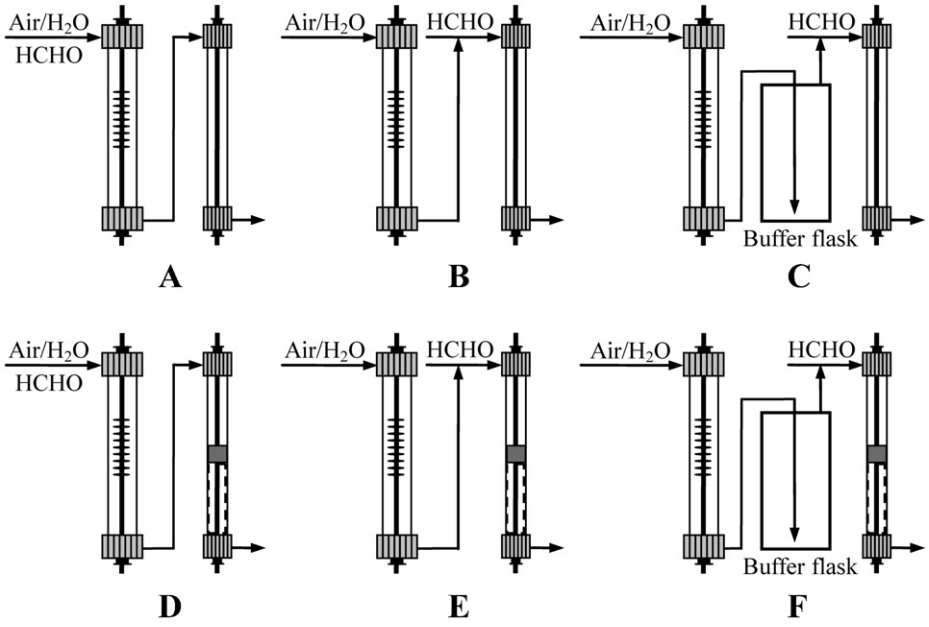

Fig. 2. Schematic diagram of the treatment systems: (A) in-plasma; (B) post-plasma; (C) ozone; (D) in-plasma + catalyst; (E) post-plasma + catalyst; (F) ozone + catalyst.

where U is the applied voltage (kV) measured with a high voltage probe (NISSIN EP-50K); I is the discharge current (mA) calculated by measuring the voltage across a 10 Ω resistor with a multimeter; Q is the flow rate of the reaction gas (L/min); 30 is the molar mass of HCHO (g/mol); 24.4 is the molar volume of gas (L/mol) under the ambient condition (around 298 K); and 60 and 3.6 are the unit conversion coefficients.

3. Results and discussion

3.1. HCHO conversion

Fig. 3 summarizes the conversion of HCHO as a function of SIE for treatment systems A, B, and D–F. The conversion was measured after the reaction reached the steady state. No HCHO conversion was observed in system C up to an SIE of 100 J/L in this study, although comparable O_3 was detected at the outlet of system C to those of systems A and B. This result validates that the reaction of HCHO with O_3 in gas phase is negligible [22]. As seen from Fig. 3, no HCHO conversion occurred without discharge power (SIE = 0) whether the catalyst was introduced or not, showing that discharge plasma is indispensable for the removal of HCHO. The MnO_x/Al_2O_3 catalyst cannot be activated for HCHO oxidation under ambient conditions.

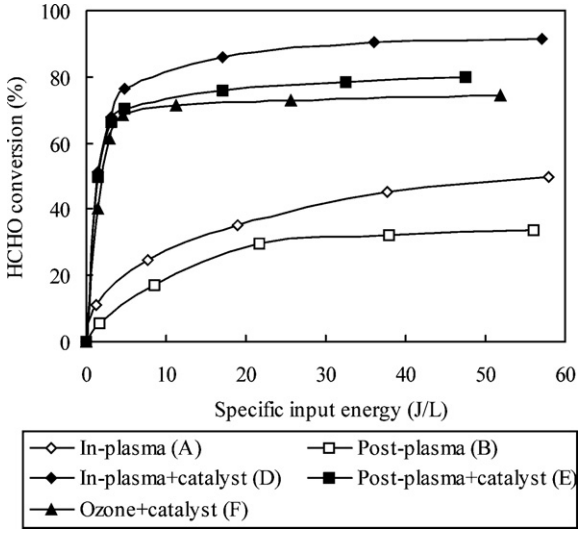

Fig. 3. Effects of specific input energy on the HCHO conversion.

For all the five treatment systems, the HCHO conversion increased with the increase of SIE. And compared with plasma alone (systems A and B), the presence of post-plasma MnO_x/Al_2O_3 catalyst (systems D–F) significantly enhances the removal of HCHO. The HCHO conversion for different systems is in the order of D > E > F ≫ A > B under the same SIE.

3.1.1. Plasma conversion of HCHO

Generally, VOCs can be removed by discharge plasma via three pathways, i.e., direct electron impacts, gas-phase radical attacks and ion collisions. Results presented in Fig. 3 show that HCHO can be removed not only in the plasma zone (system A), but also in the post-plasma cylinder (system B). For an SIE of 20 J/L, the conversion of HCHO was 36% and 29% for systems A and B, respectively.

Considering that unstable plasma species, such as energetic electrons and some gas-phase radicals, cannot reach the post-plasma reactor because of their millisecond lifetimes [23,24], the removal of HCHO in system B can only be attributed to relatively stable (not including O_3) and/or metastable plasma species (e.g. N_2 metastable states). In fact, it has been reported that for plasma removal of HCHO, N_2 metastable states may be more important than electrons owing to their longer lifetime [25]. These excited states of N_2 contribute to the removal of HCHO via two possible pathways: direct attacks towards HCHO molecules and indirect reactions through the O_2 dissociation processes, as shown in Eqs. (5)–(9) [25,26].

$$N_2(A^3\Sigma_u^+) + HCHO \rightarrow H + HCO + N_2 \quad (5)$$

$$N_2(a') + HCHO \rightarrow H + HCO + N_2 \quad (6)$$

$$N_2(A^3\Sigma_u^+) + O_2 \rightarrow O(^3P) + O(^3P) + N_2 \quad (7)$$

$$N_2(a') + O_2 \rightarrow O(^3P) + O(^3P) + N_2 \quad (8)$$

$$O + HCHO \rightarrow OH + HCO \quad (9)$$

where $N_2(a')$ denotes the three states of $a'^1\Sigma$, $a^1\Pi$ and $\omega^1\Delta$, with a mean energy of 8.4 eV; while the energy of $N_2(A^3\Sigma_u^+)$ is 6.2 eV for the $\upsilon = 0$ level.

In the case of system A in this study, besides the efficient removal of HCHO in the discharge zone, further removal of the unreacted HCHO can be expected in the downstream cylinder too, due to the residual long-living plasma-excited species.

3.1.2. Plasma-catalytic conversion of HCHO

As shown in Fig. 3, HCHO can be more efficiently removed in the plasma–catalyst hybrid systems (D–F) when compared with the plasma alone processes (systems A and B). For an SIE of 20 J/L, the conversion of HCHO was 87%, 76% and 72% for systems D, E and F, respectively. This result suggests that the downstream MnO_x/Al_2O_3 catalyst can be effectively activated by long-living plasma species for HCHO conversion at room temperature and the heterogeneous oxidation reactions over the catalyst surface are much more important for HCHO removal than the homogeneous reactions in the discharge zone.

As stated previously, not only short-living unstable reactive species are produced in plasma discharges, a fraction recombines to form more stable species such as O_3 [21,27]. Comparison of the HCHO conversion in systems C and F shows that although O_3 does not oxidize HCHO in the gas phase, it does initiate the removal of HCHO over the MnO_x/Al_2O_3 catalyst. O_3 catalytic decomposition mechanism research shows that O_3 decomposition over manganese oxide catalyst produces atomic oxygen and peroxide as the intermediate species [28,29]. These highly active oxygen species should be mainly responsible for the catalytic oxidation of HCHO in system F.

Besides O_3, other long-living plasma-excited species, which account for the HCHO removal in system B, can also exist in the second cylinder of system E. These species may trigger both homogeneous and heterogeneous reactions of HCHO, resulting in higher HCHO conversion in system E than in system F under the same conditions.

The test results in Fig. 3 also show that the treatment system D behaves the best in terms of HCHO conversion in this study, which can be easily attributed to the best use of the plasma-generated active species in a two-stage HCHO destruction process: firstly, HCHO was attacked by energetic electrons and reactive species in the discharge zone; secondly, unreacted HCHO from the discharge zone was further removed in the post-plasma stage mainly via catalytic processes initiated by O_3 and also other long-living active species.

Comparison of the HCHO conversion in systems D, E and F shows that the O_3 initiated catalytic oxidation reactions play a significant role in the plasma-catalytic removal of HCHO. Moreover, it should be noticed that for the three hybrid systems, the difference in HCHO conversion is not significant for an SIE lower than 3 J/L. We may have to consider that this phenomenon occurs for the following reasons. On the one hand, the production of high-energy long-living species, such as $N_2(A^3\Sigma_u^+)$ and $N_2(a')$, is very limited in low-energy discharge plasma. Therefore, the conversion of HCHO in system E may only result from the catalytic ozonation process just as that in system F. On the other hand, it can be seen from Fig. 3 that the heterogeneous reactions are much more important than the homogeneous reactions towards HCHO conversion, especially in the case of low SIE. This probably explains the small difference in HCHO conversion between systems D and E. Nevertheless, the difference in HCHO conversion among the three hybrid systems becomes remarkable at higher SIE, with the increasing production of high-energy long-living species and also higher HCHO conversion in the discharge zone.

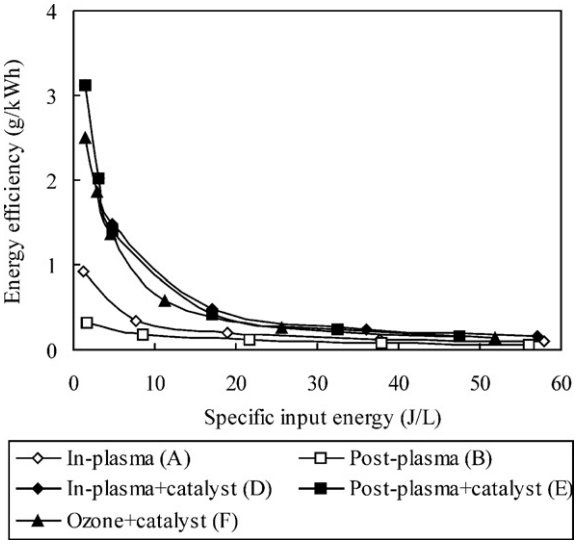

Fig. 4. Effects of specific input energy on the energy efficiency concerning HCHO conversion.

In summary, HCHO can be removed not only by short-living active species in the discharge zone, but also by long-living species except O_3 downstream the plasma reactor. Compared with the plasma alone processes, the tandem plasma–catalyst hybrid systems perform much better in HCHO conversion, mainly arising from the O_3 initiated heterogeneous destruction of HCHO over the post-plasma MnO_x/Al_2O_3 catalyst.

3.2. Energy efficiency

Fig. 4 presents the energy efficiency concerning HCHO conversion as a function of SIE for treatment systems A, B, and D–F. It can be seen that the energy efficiency decreased with the increase of SIE for all the five treatment systems. Obviously, the concentration of HCHO in the gas stream decreased with the increase of HCHO conversion, resulting in lower collision probability between HCHO molecules and active species and hence lower removed amount of HCHO per kWh of energy consumption at higher SIE. Meanwhile, more of the energy in plasma was converted into heat, photons, and used for byproduct formation (as shown in Fig. 5) with the increase of SIE. Higher SIE favors the complete removal of HCHO (Fig. 3) but causes serious energy inefficiency of the process. Therefore, maximum available value for input power in the plasma reactor will be determined not only by HCHO conversion but also by the

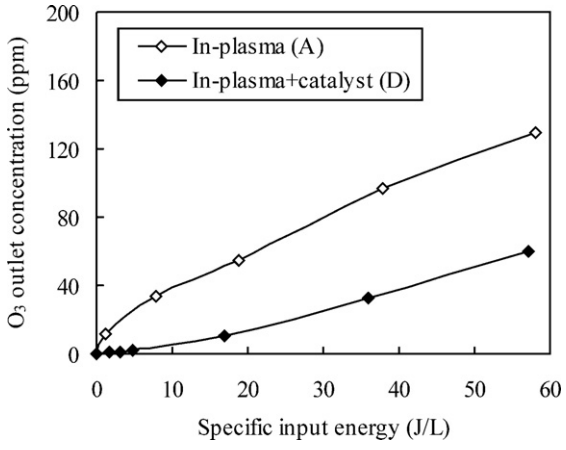

Fig. 5. Effects of specific input energy on the emission of O_3.

energy efficiency. Nevertheless, compared with the plasma alone processes (systems A and B), the energy efficiency was greatly improved by introducing post-plasma MnO_x/Al_2O_3 catalyst (systems D–F), indicating that the plasma-catalysis hybrid processes have higher HCHO removal capability and are more promising for practical applications. The maximum energy efficiency was 3.1, 3.1 and 2.5 g/kWh for systems D, E and F, respectively, compared to 0.9 g/kWh for system A and 0.3 g/kWh for system B.

3.3. Byproduct formation

3.3.1. Ozone

As long as the NTP process is operated in air-like mixtures, the formation of O_3, a hazardous discharge byproduct, is unavoidable. Fig. 5 shows the O_3 outlet concentration as a function of SIE for treatment systems A and D. In fact, O_3 outlet concentrations were measured in both the presence and absence of HCHO in air in this study for all treatment systems. Results prove that low levels of HCHO in the gas stream as well as the introduction of a buffer flask hardly influence the O_3 outlet concentration.

As seen from Fig. 5, the O_3 outlet concentration increased with the increase of SIE for both plasma alone and plasma-catalysis hybrid processes. Compared with plasma alone, however, the presence of post-plasma MnO_x/Al_2O_3 catalyst significantly reduced the O_3 emission. For an SIE of 20 J/L, the O_3 outlet concentration decreased from 57.2 ppm for system A to 13.9 ppm for system D. It is clear that mainly O_3 induced by gas discharge was decomposed catalytically over the MnO_x/Al_2O_3 surface, producing highly active oxygen species which play a key role in the enhanced removal of HCHO in the plasma-catalysis hybrid processes (Fig. 3).

Nevertheless, it should be noticed that even in the presence of MnO_x/Al_2O_3 catalyst, the O_3 emission (13.9 ppm for an SIE of 20 J/L) is still high. In future research, it will be tested if the simultaneous catalytic removal of HCHO and O_3 can be further improved by introducing catalysts that are more reactive towards O_3 decomposition.

3.3.2. Formic acid

Formic acid (HCOOH) is a common intermediate produced during the HCHO oxidation process [5,22]. Outlet concentrations of HCOOH were measured for treatment systems A and D in this study to investigate the influence of downstream MnO_x/Al_2O_3 catalyst on the formation of decomposition byproducts. In order to obtain measurable concentrations of HCOOH, a higher initial HCHO concentration of 40.9 ± 0.5 ppm was used. Fig. 6a and b shows the outlet concentration and the yield of HCOOH as functions of SIE, respectively.

As seen from Fig. 6a, the HCOOH concentration at the outlet of system A increased with the increase of SIE, indicating that HCOOH was indeed produced as a byproduct in the plasma decomposition of HCHO and the absolute production of HCOOH increased with the increase of HCHO removed at higher SIE. On the contrary, the HCOOH outlet concentration of system D linearly decreased with the increase of SIE and was much lower than that of system A under the same SIE. For an SIE of 80 J/L, the HCOOH outlet concentration was 2.0 and 0.1 ppm for systems A and D, respectively. The difference in HCOOH production between the two systems indicates that HCOOH produced in the discharge zone can be effectively removed over the downstream MnO_x/Al_2O_3 catalyst, especially at higher SIE. The presence of post-plasma MnO_x/Al_2O_3 catalyst does not only significantly enhance the conversion of HCHO (Fig. 3), but also favors the elimination of organic byproducts.

In addition, results presented in Fig. 6b show that the HCOOH yield decreased with the increase of SIE for both systems A and D. Since the absolute removal of HCHO increased with the increase of SIE, the decreasing HCOOH yield in system D can be easily attributed to its decreasing production of HCOOH, as shown in Fig. 6a. On the other hand, although the production of HCOOH increased with the increase of SIE in system A (Fig. 6a), the HCOOH yield decreased monotonously, suggesting that more of the removed HCHO tends to undergo further oxidation reactions in higher-energy discharge plasma to form end products such as CO_2 and CO.

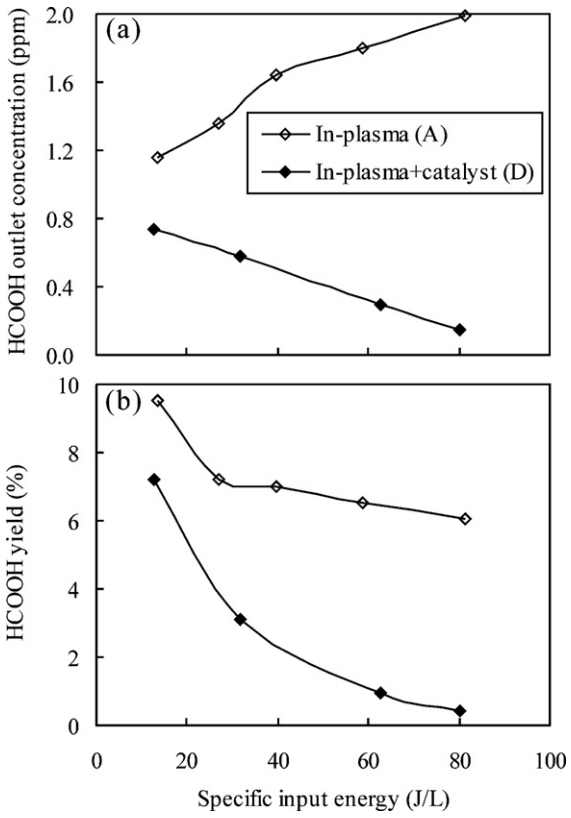

Fig. 6. Effects of specific input energy on the production of HCOOH: (a) HCOOH concentration and (b) HCOOH yield.

4. Conclusions

The roles of various plasma species in the plasma and plasma-catalytic removal of low-concentration HCHO in air were experimentally studied in this work. The main findings can be summarized as follows:

(1) Both short- and long-living plasma species (other than O_3) contribute to HCHO removal in the gas phase.
(2) O_3 does not initiate HCHO removal in the gas phase but does trigger heterogeneous destruction of HCHO over the MnO_x/Al_2O_3 catalyst, well explaining the greatly enhanced HCHO conversion by combining plasma with the MnO_x/Al_2O_3 catalyst in series.
(3) The best use of plasma-generated active species for HCHO destruction can be achieved in a plasma–catalyst hybrid system where HCHO is introduced through the discharge zone and then the catalyst bed, leading to the highest energy efficiency concerning HCHO conversion.
(4) The introduction of MnO_x/Al_2O_3 catalyst after the plasma reactor significantly reduces the emission of discharge byproducts (O_3) and organic intermediates (HCOOH), showing great potential for indoor VOCs' purification.

Acknowledgement

The authors thank the National High Technology Research and Development Program (863) of China (No. 2010AA064904) for the financial support of this work.

References

[1] T. Salthammer, S. Mentese, R. Marutzky, Formaldehyde in the indoor environment, Chem. Rev. 110 (2010) 2536–2572.
[2] D.A. Missia, E. Demetriou, N. Michael, E.I. Tolis, J.G. Bartzis, Indoor exposure from building materials: a field study, Atmos. Environ. 44 (2010) 4388–4395.
[3] X.J. Tang, Y. Bai, A. Duong, M.T. Smith, L.Y. Li, L.P. Zhang, Formaldehyde in China: production, consumption, exposure levels, and health effects, Environ. Int. 35 (2009) 1210–1224.
[4] S. Tanada, N. Kawasaki, T. Nakamura, M. Araki, M. Isomura, Removal of formaldehyde by activated carbons containing amino groups, J. Colloid Interface Sci. 214 (1999) 106–108.
[5] F. Shiraishi, D. Ohkubo, K. Toyoda, S. Yamaguchi, Decomposition of gaseous formaldehyde in a photocatalytic reactor with a parallel array of light sources. 1. Fundamental experiment for reactor design, Chem. Eng. J. 114 (2005) 153–159.
[6] C.B. Zhang, H. He, K.I. Tanaka, Perfect catalytic oxidation of formaldehyde over a Pt/TiO_2 catalyst at room temperature, Catal. Commun. 6 (2005) 211–214.
[7] X.F. Tang, J.L. Chen, Y.G. Li, Y. Li, Y.D. Xu, W.J. Shen, Complete oxidation of formaldehyde over Ag/MnO_x–CeO_2 catalysts, Chem. Eng. J. 118 (2006) 119–125.
[8] C.Y. Li, Y.N. Shen, M. Jia, S.S. Sheng, M.O. Adebajo, H.Y. Zhu, Catalytic combustion of formaldehyde on gold/iron-oxide catalysts, Catal. Commun. 9 (2008) 355–361.
[9] R.H. Wang, J.H. Li, OMS-2 catalysts for formaldehyde oxidation: effects of Ce and Pt on structure and performance of the catalysts, Catal. Lett. 131 (2009) 500–505.
[10] J. Van Durme, J. Dewulf, W. Sysmans, C. Leys, H. Van Langenhove, Efficient toluene abatement in indoor air by a plasma catalytic hybrid system, Appl. Catal. B: Environ. 74 (2007) 161–169.
[11] M. Schiorlin, E. Marotta, M. Rea, C. Paradisi, Comparison of toluene removal in air at atmospheric conditions by different corona discharges, Environ. Sci. Technol. 43 (2009) 9386–9392.
[12] E. Marotta, A. Callea, M. Rea, C. Paradisi, DC corona electric discharges for air pollution control. Part 1. Efficiency and products of hydrocarbon processing, Environ. Sci. Technol. 41 (2007) 5862–5868.
[13] M.B. Chang, C.C. Lee, Destruction of formaldehyde with dielectric barrier discharge plasmas, Environ. Sci. Technol. 29 (1995) 181–186.
[14] A. Ogata, H. Einaga, H. Kabashima, S. Futamura, S. Kushiyama, H. Kim, Effective combination of nonthermal plasma and catalysts for decomposition of benzene in air, Appl. Catal. B: Environ. 46 (2003) 87–95.
[15] H.X. Ding, A.M. Zhu, F.G. Lu, Y. Xu, J. Zhang, X.F. Yang, Low-temperature plasma-catalytic oxidation of formaldehyde in atmospheric pressure gas streams, J. Phys. D: Appl. Phys. 39 (2006) 3603–3608.
[16] Y.F. Guo, X.B. Liao, J.H. He, W.J. Ou, D.Q. Ye, Effect of manganese oxide catalyst on the dielectric barrier discharge decomposition of toluene, Catal. Today 153 (2010) 176–183.
[17] X. Fan, T.L. Zhu, M.Y. Wang, X.M. Li, Removal of low-concentration BTX in air using a combined plasma catalysis system, Chemosphere 75 (2009) 1301–1306.
[18] X. Fan, T.L. Zhu, Y.J. Wan, X. Yan, Effects of humidity on the plasma-catalytic removal of low-concentration BTX in air, J. Hazard. Mater. 180 (2010) 616–621.
[19] H.L. Chen, H.M. Lee, S.H. Chen, M.B. Chang, S.J. Yu, S.N. Li, Removal of volatile organic compounds by single-stage and two-stage plasma catalysis systems: a review of the performance enhancement mechanisms, current status, and suitable applications, Environ. Sci. Technol. 43 (2009) 2216–2227.
[20] A.M. Harling, D.J. Glover, J.C. Whitehead, K. Zhang, The role of ozone in the plasma-catalytic destruction of environmental pollutants, Appl. Catal. B: Environ. 90 (2009) 157–161.
[21] W.J. Liang, J. Li, J.X. Li, T. Zhu, Y.Q. Jin, Formaldehyde removal from gas streams by means of $NaNO_2$ dielectric barrier discharge plasma, J. Hazard. Mater. 175 (2010) 1090–1095.
[22] K. Hensel, J. Pawlat, K. Takashima, A. Mizuno, Possibilities of formaldehyde removal by discharge plasma, in: Proceedings of the International Joint Power Generation Conference, Atlanta, GA, USA, June 16–19, 2003, pp. 803–807.
[23] K. Urashima, J.S. Chang, Removal of volatile organic compounds from air streams and industrial flue gases by non-thermal plasma technology, IEEE Trans. Dielectr. Electr. Insul. 7 (2000) 602–614.
[24] N.Q. Yan, Z.C. Wu, T.E. Tan, Modeling of formaldehyde destruction under pulsed discharge plasma, J. Environ. Sci. Health A 35 (2000) 1951–1964.
[25] N. Blin-Simiand, S. Pasquiers, F. Jorand, C. Postel, J.R. Vacher, Removal of formaldehyde in nitrogen and in dry air by a DBD: importance of temperature and role of nitrogen metastable states, J. Phys. D: Appl. Phys. 42 (2009), doi:10.1088/0022-3727/42/12/122003.
[26] H.X. Ding, A.M. Zhu, X.F. Yang, C.H. Li, Y. Xu, Removal of formaldehyde from gas streams via packed-bed dielectric barrier discharge plasmas, J. Phys. D: Appl. Phys. 38 (2005) 4160–4167.
[27] J. Van Durme, J. Dewulf, C. Leys, H. Van Langenhove, Combining non-thermal plasma with heterogeneous catalysis in waste gas treatment: a review, Appl. Catal. B: Environ. 78 (2008) 324–333.
[28] W. Li, S.T. Oyama, Mechanism of ozone decomposition on a manganese oxide catalyst. 2. Steady-state and transient kinetic studies, J. Am. Chem. Soc. 120 (1998) 9047–9052.
[29] W. Li, G.V. Gibbs, S.T. Oyama, Mechanism of ozone decomposition on a manganese oxide catalyst. 1. In situ Raman spectroscopy and ab initio molecular orbital calculations, J. Am. Chem. Soc. 120 (1998) 9041–9046.